



# Tracking the global flows of atmospheric moisture

Obbe A. Tuinenburg<sup>1,2,3</sup>, Arie Staal<sup>2,3</sup>

<sup>1</sup> Copernicus Institute for Sustainable Development, Utrecht University, Utrecht, 3508 TC, the Netherlands

<sup>2</sup> Stockholm Resilience Centre, Stockholm University, Stockholm, SE-10691, Sweden

5 <sup>3</sup> Bolin Centre for Climate Research, Stockholm, SE-10691, Sweden

*Correspondence to:* Obbe A. Tuinenburg (o.a.tuinenburg@uu.nl)

**Abstract.** Many processes in hydrology and Earth system science relate to moisture recycling, the contribution of terrestrial evaporation to precipitation. For example, the effects of land-cover changes on regional rainfall regimes depend on this process. To study moisture recycling, a range of moisture tracking models are in use that are forced with output from atmospheric models, but differ in various ways. They can be Eulerian (grid-based) or Lagrangian (trajectory-based), have two or three spatial dimensions, and rely on a range of other assumptions. Which model is most suitable depends on the purpose of the study, but also on the quality and resolution of the data with which it is forced. Recently, the high-resolution ERA5 reanalysis dataset has become the state-of-the-art, paving the way for a new generation of moisture tracking models. However, it is unclear how the new data can best be used to obtain accurate estimates of atmospheric moisture flows. Here we develop a set of moisture tracking models forced with ERA5 data and systematically test their performance regarding continental evaporation recycling ratio, distances of moisture flows, and ‘footprints’ of evaporation from seven point sources across the globe. We report simulation times to assess possible trade-offs between accuracy and speed. Three-dimensional Lagrangian models were most accurate and ran faster than Eulerian versions for tracking water from single grid cells. The rate of vertical mixing of moisture in the atmosphere was the greatest source of uncertainty in moisture tracking. We conclude that the recently improved resolution of atmospheric reanalysis data allows for more accurate moisture tracking results in a Lagrangian setting, but that considerable uncertainty regarding turbulent mixing remains. We present an efficient Lagrangian method to track atmospheric moisture flows from any location globally using ERA5 reanalysis data and make the code for this model publicly available.

## 1 Introduction

25 Moisture recycling is the process in which continental evaporation re-precipitates on land (Fig. 1), which is increasingly well understood and recognized as an important process in the Earth system. As a mechanism linking remote areas on the planet, it affects how land-cover changes influence regional precipitation (Spracklen et al., 2018), how droughts may or may not spatially propagate (Zemp et al., 2014), and whether continental interior areas receive enough precipitation for agriculture (Keys et al., 2016). With the growing interest in the topic and with increasing data availability, moisture recycling models are being used to address a wider range of questions and on higher spatial and temporal detail. Examples include the regional hydroclimatic

30



effects of deforestation in the Amazon (Staal et al., 2018) and the dependency of cities' water supply on upwind land areas (Keys et al., 2018).

35 In moisture recycling model studies, moisture is tracked through the atmosphere. This is generally done using an 'offline' model; all such models share some features, but also differ in notable ways. Universal approaches and principles among offline moisture tracking models is that they apply the atmospheric water balance (Burde and Zangvil, 2001), they run *a posteriori* using atmospheric reanalysis data or other atmospheric model output (Van der Ent et al., 2013), and at each time step, the atmospheric moisture budget is updated based on wind, evaporation, and precipitation estimates. Their output, therefore, quantifies estimates of water transfer among any combination of locations or areas on Earth (Fig. 1).

40 The most notable way in which moisture tracking models differ is in their representation of space. The models can be categorized into Eulerian models, which are grid-based, and Lagrangian models, which are trajectory-based. In Eulerian models, moisture flows between discrete grid cells at each time step; in Lagrangian models, individual particles have a location with coordinates that are updated at each time step (Fig. 2).

45 Besides assumptions regarding their grid representation (Eulerian or Lagrangian), all studies that use offline moisture tracking models make assumptions regarding vertical mixing of the moisture at the start of the tracking and during its path through the atmosphere, integration time step, interpolation, and resolution of the forcing dataset. In each moisture recycling study, assumptions are chosen such that a suitable trade-off is achieved between accuracy of the representation of the downwind moisture footprint of evaporation, amount of data needed, and simulation time (Van der Ent et al., 2013). For example, in Eulerian models, the grid-cell size may be determined by available data, but the integration time step is not. If an explicit numerical scheme is used and the moisture flows within a single time step are much larger or smaller than the length of the grid cell, the model will give incorrect results due to numerical inaccuracies. The advantage of using a Eulerian model, however, is that it is relatively fast for simulations in which moisture is released from a large fraction of the globe. In Lagrangian models, a larger number of particles released per unit of evaporation increases the computing time, making it beneficial to minimize the number of tracked particles. However, if this number is chosen too small, the simulation is unable to capture atmospheric moisture convergence and divergence. In both Lagrangian and Eulerian models, the modeller should determine the optimal values to minimize errors.

60 Often, assumptions and uncertainties in moisture recycling studies are not reported. However, until now, data limitations constrained certain choices such as the minimal spatial resolution, which prevented Courant numbers exceeding one in Eulerian models. Many recent moisture recycling studies have used ERA-Interim reanalysis data (Van der Ent et al., 2010; Van der Ent and Savenije, 2011; Tuinenburg et al., 2012; Zemp et al., 2014, 2017; Staal et al., 2018; Wang-Erlandsson et al., 2018), with a temporal resolution of six hours and a spatial resolution of  $0.75^\circ$  (Dee et al., 2011), as their forcing data. However, with the



65 recent replacement of ERA-Interim by the ERA5 dataset, which has a temporal resolution of one hour and a spatial resolution  
of  $0.25^\circ$ , the trade-offs caused by the assumptions in the moisture recycling models may have shifted. The drawback of using  
higher-resolution data is that moisture tracking becomes more data-intensive and computing times may increase significantly.  
We here assess the trade-offs and sensitivities in various atmospheric moisture recycling models forced by ERA5 reanalysis  
70 moisture flows can best be represented given the quality of the presently available reanalysis data. Specifically, we test the  
sensitivities of downwind precipitation locations to potentially important model assumptions for tracking the evaporation from  
seven point locations across the globe. These assumptions relate to model structure, forcing data resolution, number of tracked  
particles, interpolation, and model time step. We evaluate the different model version based on a number of hydrologically  
relevant variables: continental evaporation recycling ratio (the percentage of evaporation that rains down over land), mean  
75 absolute latitudinal distance of the moisture transport, mean absolute longitudinal distance, and mean latitudinal and  
longitudinal change of the tracked moisture. We hypothesize that a Eulerian representation of the atmosphere at the resolution  
of ERA5 causes deviations in these variables from Lagrangian model versions. We also hypothesize that the improved  
resolution of vertical wind speeds allows for more accurate moisture recycling estimates, causing those estimates to deviate  
more with the vertical degradation of the data. Altogether, our analyses present model-dependent uncertainties in moisture  
80 recycling estimates across the globe. Based on our results we develop a moisture tracking model for ERA5 reanalysis data  
with optimal model assumptions and make it available on Github.

## 2 Methods

This paper tests the sensitivity in atmospheric moisture recycling to different assumptions in atmospheric moisture recycling  
models. In Section 2.1 we discuss the common principles of the model versions tested in this study and their differences  
85 regarding model structure and assumptions. In Section 2.2 we discuss the different simulation options that were tested.

### 2.1 Model descriptions

The offline atmospheric moisture recycling models used in this study are employed to determine the next precipitation location  
of evaporation that enters the atmosphere. This is done by using ERA5 atmospheric reanalysis as forcing data (Copernicus  
Climate Change Service), and effectively use the moisture tracking model as post-processing to this reanalysis. In general,  
90 atmospheric moisture tracking is achieved by following moisture along its path through the atmosphere and keeping track of  
how much of that moisture rains out where. For example, a given amount of moisture enters the atmosphere through  
evaporation at some moment and location. Once the moisture is in the atmosphere, its downwind transport is tracked with the  
wind fields from the forcing data. Until precipitation has occurred at the location of the moisture, all the moisture remains in  
the atmosphere. However, once there is precipitation, a fraction of the moisture (precipitation over precipitable water,  $\frac{P}{PW}$ ) that  
95 is still present in the atmosphere is allocated to rain out in that location. Thus, the fraction of the original evaporation remaining



in the atmosphere decreases with downwind moisture transport. In this study, the evaporated moisture is tracked until 99% of the moisture is allocated, or the moisture has been in the atmosphere for 30 days, whichever comes first.

100 Despite these communalities between the model versions, several important assumptions are made that potentially affect the path of moisture through the atmosphere. These are discussed in the rest of this section.

### 2.1.1 Eulerian and Lagrangian model versions

105 Atmospheric moisture tracking models are used in either a Eulerian setting (Yoshimura et al., 2004; Dominguez et al., 2006; Van der Ent et al., 2010, 2013; Goessling and Reick, 2011; Singh et al., 2016) or a Lagrangian setting (Stohl et al., 2005; Dirmeyer and Brubaker, 2007; Tuinenburg et al., 2012). In a Eulerian model, the atmosphere through which the evaporated moisture is transported is divided into grid boxes, which may be the same size as the forcing data, but may also be coarser than the forcing data, such as in WAM-2layers (Van der Ent et al., 2014), which typically runs on 1.5° resolution. This means that moisture can only flow from one grid cell to one of its direct neighbours, which may be problematic if the time step is either too large or too small relative to the moisture flows between neighbouring cells. If this time step is chosen too large, real moisture transport may occur faster than the simulation grid and time step allow for (i.e., if the Courant number  $C = \frac{v\Delta t}{\Delta x} > 1$ ).  
110 If the time step is taken too small, numerical diffusion will occur, meaning that moisture transport in the model will be faster than in the forcing data.

In a Lagrangian model, the internal model state is not a model grid, but instead a collection of water particles. During the simulation, these water particles are released and advected with the forcing wind field. The location of the particles is not bound to the grid of the forcing data, which means that the Lagrangian model can accommodate large atmospheric moisture fluxes, i.e. particles can jump several grid cells of the forcing data in one model time step. The advantage of Lagrangian models is that these do not suffer from the potential numerical inaccuracies of the Eulerian models, and therefore better resemble the moisture transport in the forcing data. The simulation time of Lagrangian models scales with the number of particles released, which is low for point releases but high if evaporation from large areas is considered.

### 120 2.1.2 Two-dimensional vs Three-dimensional simulations

For both the Eulerian and the Lagrangian model versions we perform simulation with two- and three-dimensional forcing data in order to test the influence of the vertical variability of atmospheric moisture flows on the moisture tracking results. When the model is forced with three-dimensional data, the horizontal (north/south, which is “northward” in ERA5, and east/west, which is “eastward” in ERA5) transport is driven by the wind speed at the pressure level of the particle (Lagrangian model) or grid cell (Eulerian model). For both models, we release the moisture in the lowest grid box or just above the surface. During  
125 the simulation, there is perfect vertical mixing every 24 hours. For the Lagrangian simulation, this means that the particle will



be displaced vertically to a random altitude, weighed with the local moisture profile on average every 24 hours (see Section 2.1.4). For the Eulerian simulations, the tracked moisture is distributed vertically proportional to the local moisture profile every 24 hours.

130

In case of forcing with two-dimensional data, there is no vertical variability in horizontal transport. The horizontal transport is then driven by the vertical integral of eastward and northward moisture transport divided by the precipitable water times the grid cell length in the direction of transport.

135 All following experiments were carried out with the three-dimensional Lagrangian model version.

### 2.1.3 Release height of moisture entering the atmosphere

We also test the differences between releasing moisture from the surface and releasing it well-mixed in the atmospheric column. Naturally, actual evaporation occurs at the surface, but moisture tracking simulations generally assume a well-mixed starting condition, which may affect the precipitation footprints of evaporation sources (Bosilovich, 2002). For the three-dimensional simulations, the initial vertical position of the moisture entering the atmosphere has to be determined. For the Eulerian simulation, we add the moisture to the lowest vertical level, just above the surface. For the Lagrangian simulations, there are two options. Either the particles are released just above the surface as in the Eulerian simulations, or the particles are released at a random vertical location weighted by the local vertical humidity profile, as in (Dirmeyer and Brubaker, 2007).

140

### 2.1.4 Vertical displacement during transport

For the three dimensional Lagrangian simulations, the vertical location of the moisture particles has to be updated during the atmospheric transport. We test several options for this vertical displacement. The first option is to use the ERA5 large-scale vertical wind speed, ‘omega’, for the vertical displacement. Due to all kinds of sub-grid processes, such as convection, turbulence etc., omega is almost certainly an underestimation of air mixing in the vertical direction. However, the extent to which this occurs and affects moisture recycling is unknown. Hence, apart from using omega as the input for vertical displacement, we also explore options where each parcel of moisture has a certain probability of being assigned a random new vertical position scaled by the local vertical moisture profile. This is the same procedure used to determine the initial vertical position as in (Dirmeyer and Brubaker, 2007). This means that moisture particles can potentially have a quite strong vertical displacement in a short time. However, this may be realistic if the particle is part of a convective up- or downdraft. During every time step, there is a small probability of running the vertical displacement. We summarize these stochastic vertical displacement versions of the model by the average time for one repositioning of one parcel, which is once per hour, once per six hours, once per 24 hours and once per 120 hours.

150

155



## 2.2 Experimental set-up

### 2.2.1 Forcing data and simulations

We force the moisture tracking models with ERA5 hourly atmospheric reanalysis data on  $0.25 \times 0.25^\circ$  resolution. We use two-dimensional fields of Total Precipitation, Evaporation, Vertical integral of northward water vapour flux, Vertical integral of eastward water vapour flux and Total Column Water Vapour and three-dimensional fields of Specific Humidity, U and V components of wind speed and Vertical wind speed. For the three-dimensional fields, we use data on 25 pressure levels: every 25 hPa between 1000 hPa and 750 hPa, and every 50 hPa between 750 hPa and 50 hPa, except for the simulations with degraded forcing data (see 2.2.2). For the Eulerian model setup, we use the same grid setup as the ERA5 forcing data, which is  $0.25^\circ$  spatial resolution and—for a three dimensional simulation—25 vertical layers.

For this study, we track evaporation that enters the atmosphere in the first five days of July 2012. We continue to track this moisture either until it has all been allocated, or the simulation reaches the end of July 2012. We perform forward tracking from seven point sources around the world with different climates and topographies: Chendu in China ( $30.75^\circ\text{N}$ ,  $103.5^\circ\text{E}$ ), Central Kansas in the USA ( $39.0^\circ\text{N}$ ,  $86.0^\circ\text{W}$ ), Manaus in Brazil ( $3.0^\circ\text{S}$ ,  $60.0^\circ\text{W}$ ), Nagpur in India ( $20.0^\circ\text{N}$ ,  $80.0^\circ\text{E}$ ), Nairobi in Kenya ( $1.25^\circ\text{S}$ ,  $36.75^\circ\text{E}$ ), Stockholm in Sweden ( $59.5^\circ\text{N}$ ,  $18.0^\circ\text{E}$ ), and Utrecht in the Netherlands ( $52.0^\circ\text{N}$ ,  $5.0^\circ\text{E}$ ). We carry out experiments in which we evaluate the model output based on a number of criteria: visual difference in footprint, the continental recycling ratio (the percentage of evaporation that rains down over land; CRR), mean absolute latitudinal distance of the moisture transport, mean absolute longitudinal distance, and mean latitudinal and longitudinal change of the moisture. Despite the fact that simulation times are very much CPU dependent, we give an estimation of the simulation time necessary (excluding the reading of the forcing data from disk). We compare the results against a baseline model that incorporates as much detail as is possible given the available data: a 3D Lagrangian model with interpolated wind speeds and directions, with the high amount of released 10,000 particles per mm of evaporation.

We show the results for Manaus in the main text and add figures for footprints of the other locations in the Supplementary Material.

### 2.2.2 Vertical degradation of the forcing data

The number of vertical layers can have a strong effect on the outcome (Van der Ent et al., 2013), but this has never been tested with the large amount of vertical layers (137 model levels, but output is available on 37 pressure levels, of which this study uses 25) in ERA5. Since the size of the forcing data is substantial on full resolution (around 200 Gb for one month of forcing data), we are interested in determining the degradation of the results if we degrade the vertical resolution of the forcing data. As alternatives to non-degraded data, we consider six degradations of the forcing data, consisting of two sets of three degradations. In the first set, we use the full atmospheric column, but reduce the vertical resolution to 50 hPa ( $^{\circ}\text{hpa}50^{\circ}$ ), 100



hPa ('hpa100') and 200 hPa ('hpa200'). In the second set, we use only forcing data between 1000 hPa and 500 hPa, since this  
190 is where the majority of the moisture is found. The vertical resolutions of this second set are 25 hPa ('5k25'), 50 hPa ('5k50')  
and 100 hPa ('5k100').

### 2.2.3 Interpolation within the ERA5 space and time grid

If the internal model time step of the moisture tracking model is smaller than the one-hour temporal resolution of the ERA5  
forcing data set, the forcing data need to be linearly interpolated in time. For the Lagrangian model, the same is true for the  
195 spatial grid: the particles may be present on different locations than the grid cell centres of the forcing data. Therefore, linear  
interpolation on the spatial grid is done as well. As a default, all simulations in this study use linear spatial interpolation, but  
this interpolation might be costly in terms of simulation time. Therefore, we test how much accuracy is lost if the simulation  
is run without linear interpolation and the nearest neighbour value of the forcing data is used instead.

### 2.2.4 Number of particles released per unit of evaporation

200 For the Lagrangian simulations, the trajectories of the moisture that enters the atmosphere is simulated through a number of  
particles. This number has to be chosen carefully. If the moisture is simulated by a small number of particles, atmospheric  
moisture convergence and divergence cannot be simulated well enough. However, since the simulation time of the Lagrangian  
simulation scales approximately linearly with the number of particles, simulation times may increase too much if the number  
of particles chosen is too large. By default, we release 2000 moisture particles per mm of evaporation for all simulations.  
205 However, to test for the effect of different number of particles, we performed simulations with 100, 500, 2,000 and 10,000  
particles per mm and assess their differences.

### 2.2.5 Integration time step

The internal time step of the moisture tracking model can influence the simulation result. In the default simulation, it is set at  
0.1 h. If it is set at a high value, the simulation time is reduced, but the Lagrangian trajectories may become unrealistic, as the  
210 forcing data are assumed to be constant during the entire time step. However, if the time step is chosen very small, simulation  
times might increase too much with too limited improvement in accuracy. We perform simulations with internal time steps of  
0.01 h, 0.05 h, 0.1 h, 0.5 h and 1 h.

The internal time step of the Eulerian simulations is 0.1 h, ensuring numerical stability of the simulations. In ERA5, the  
215 absolute eastward wind speed divided by the grid cell size in the east-west direction can be higher than a grid cell length per  
hour (for July 2012, see Fig. S1). These values are typically larger at higher latitudes than near the equator, given the smaller  
east-west grid cell size near the poles. Moreover, these values are larger further away from the surface, as the wind speed tends  
to increase with altitude. The Courant numbers for vertically integrated eastward moisture transport divided by the precipitable  
water are generally lower than for the individual layers, but can be larger than one grid cell per hour in up to 40° of latitude



220 away from the poles (Fig. S1). This means that if the simulation time step is too large, Courant numbers are larger than unity  
and moisture cannot be correctly transported on the Eulerian grid. Since decreasing the time step prohibitively increases the  
simulation time, Eulerian simulations were only done with a time step of 0.1 h.

### 3 Results

#### 3.1 Differences between Eulerian and Lagrangian models in two and three dimensions

225 Comparing two-dimensional and three-dimensional Eulerian and Lagrangian models, we find considerable differences in the  
'footprints' of evaporation during July 2012 from our point sources across the globe. The mean difference in continental  
recycling ratio (CRR) with the baseline model across the source locations was 13 percentage points for the two-dimensional  
Eulerian model, 11 percentage points for the three-dimensional Eulerian one, 14 percentage points for the two-dimensional  
Lagrangian one, and zero percentage points for the three-dimensional Lagrangian one. The mean difference in absolute  
230 latitudinal transport distance with the baseline model was  $4.4^\circ$  for the two-dimensional Eulerian model,  $4.5^\circ$  for the three-  
dimensional Eulerian one,  $2.2^\circ$  for the three-dimensional Lagrangian one, and  $0.0^\circ$  degrees for the three-dimensional  
Lagrangian one. Similarly, the mean difference in absolute longitudinal transport distance was  $3.2^\circ$  for the two-dimensional  
Eulerian model,  $5.3^\circ$  for the three-dimensional Eulerian one,  $2.2^\circ$  for the three-dimensional Lagrangian one, and  $0.0^\circ$  degrees  
for the three-dimensional Lagrangian one.

235

Relative to the baseline model, both the two-dimensional and three-dimensional Eulerian models underestimate atmospheric  
transport distances in both latitudinal and longitudinal directions (only the absolute longitudinal transport in the case of Nagpur  
for the two-dimensional model is higher). This relatively close transport does not, however, lead to a consistent overestimation  
of CRR: for Nagpur, Nairobi and Utrecht the CRR is lower than in the baseline model (Table 1), which is due to geographical  
240 reasons (e.g. increased local flow from Nairobi to Lake Victoria, which is not regarded as continental in the ERA5 land mask).  
The simple, two-dimensional Lagrangian model tends to track moisture flows too far and therefore underestimates CRR in all  
simulations (Table 1). The three-dimensional Lagrangian model practically performs the same as the baseline model: all CRR  
estimates are equal with one percentage point accuracy. Only the absolute latitudinal distance for Utrecht and Stockholm and  
the absolute longitudinal distance for Stockholm were  $0.1^\circ$  higher than that for the baseline model (with  $0.1^\circ$  accuracy) (Table  
245 1).

The case of Manaus illustrates how differences between models can cause divergent estimates for CRR (Fig. 3). The CRR  
varies from 38% in the two-dimensional Lagrangian model to 91% in the two-dimensional Eulerian model. The continental  
recycling ratios for the three-dimensional Eulerian (76%) and three-dimensional Lagrangian (68%) models are closer to that  
250 of the baseline model (68%). The low value for the two-dimensional Eulerian model coincides with its failure to simulate  
moisture flows across the Andes (Fig. 3A). The two-dimensional Lagrangian model simulates a relatively large flow across





the Andes (Fig. 3C) followed by the three-dimensional Lagrangian model (Fig. 4D). Differences in footprints from other sources than Manaus are also substantial (Figs. S2–S7). For example, both Lagrangian models simulate a remote flow from Nairobi up to India, which is entirely absent from the simulations of the Eulerian models (Fig. S4).

255

Calculation times differ more among the four model versions than among the simulations in a single model version (Table 1). The simulations took (mean  $\pm$  standard deviation)  $2650 \pm 538$  CPU seconds with the two-dimensional Eulerian model,  $20470 \pm 610$  CPU seconds with the three-dimensional Eulerian model,  $46 \pm 16$  CPU seconds with the two-dimensional Lagrangian model,  $279 \pm 108$  CPU seconds with the three-dimensional Lagrangian model, and  $1384 \pm 538$  CPU seconds with the baseline model. In other words, for the point sources considered, the two-dimensional Lagrangian model is about 30 times faster than the baseline model, the three-dimensional Lagrangian model is five times faster, the two-dimensional Eulerian model is two times slower, and the three-dimensional Eulerian model is 15 times slower than the baseline model.

260

### 3.2 Effects of number of tracked particles

We compared the effects of tracking different amounts of particles in a three-dimensional Lagrangian model: 100, 500, 2,000 (i.e. the three-dimensional model in 3.1), and 10,000  $\text{mm}^{-1}$  evaporation  $\text{h}^{-1}$  (i.e. the baseline model). The number of particles has a small effect on the level of detail. The runs with 500 and 2,000 particles  $\text{mm}^{-1}$   $\text{h}^{-1}$  did not result in any differences with the baseline model regarding CRR, mean absolute latitudinal distance or mean absolute longitudinal distance. The runs with 100 particles  $\text{mm}^{-1}$   $\text{h}^{-1}$  resulted in a difference of  $0.1^\circ$  for both mean absolute latitudinal distance and mean absolute longitudinal distance, but no difference in CRR. It can be seen for the simulations for Manaus (Fig. 4) and the other locations (Figs. S8–S13) that the smoothness of the footprints increases with the number of tracked particles, but the figures confirm that the patterns in the baseline model are already captured by the simulations with 100 particles  $\text{mm}^{-1}$   $\text{h}^{-1}$ . The simulation times did differ considerably, because they scale roughly linearly with the number of tracked particles: the simulations with 2,000, 500, and 100 particles  $\text{mm}^{-1}$   $\text{h}^{-1}$  were on average five times, 19 times and 83 times faster than that with 10,000 particles  $\text{mm}^{-1}$   $\text{h}^{-1}$ .

265

270

### 3.3 Effects of release height

The two different ways of tracked particle release in the atmospheric column, moisture release at the surface and moisture release scaled with the vertical moisture profile, led to differences in evaporation footprints. Although the average difference in CRR between both model versions was zero percentage points, the model with moisture profile release produced more distant flows than that with surface release: for all locations it resulted in larger latitudinal flows, with an average of  $0.2^\circ$ ; for all locations except Kansas it resulted in larger longitudinal flows as well, by  $0.3^\circ$  on average (both the mean difference and mean absolute difference).

275

280



285

The footprints for the simulations with moisture profile release and surface release are visually very similar (Figs. 5, S14–S19). However, the distance of moisture transport can differ substantially, as exemplified by the mean longitudinal distance of transport from Utrecht, which differed by as much as  $0.8^\circ$  (Fig. S19).

The average calculation time for surface release was 2% faster than for moisture profile release.

### 3.4 Effects of interpolation

We find effects of interpolation of wind speeds and direction in the three-dimensional Lagrangian model on evaporation footprints. The mean absolute difference in CRR between the interpolated and non-interpolated simulations was one percentage point. For Kansas and Nagpur, estimated CRR is lower without interpolation, but in the other cases it was higher without interpolation. Because of this lack of consistent difference, the mean CRR across locations was equal for both model versions (with an accuracy of one percentage point). The absolute latitudinal distance of moisture flows was lower without interpolation, except in the case of Kansas. Both the mean difference and mean absolute difference in latitudinal distance between the two model versions were  $0.3^\circ$ . The absolute longitudinal distance of moisture flows also tended to be lower without interpolation, except in the cases of Kansas and Utrecht. The mean difference in longitudinal distance was  $0.1^\circ$ , and the mean absolute longitudinal difference  $0.3^\circ$ , between the runs with the interpolated and non-interpolated data. The simulations with interpolation were on average 3% slower than those without interpolation. Visually, the differences in evaporation footprint are very small (Figs. 6, S20–S25).

### 3.5 Effects of degraded vertical atmospheric profile

The six versions of the three-dimensional Lagrangian model with a degraded vertical atmospheric profile ('hpa50', 'hpa100', 'hpa200', '5k25', '5k50' and '5k100') yielded considerable differences in evaporation footprints and their statistics: the output from 'hpa50' differed from that of the baseline model by an average of seven percentage points in CRR, by  $1.7^\circ$  in absolute latitudinal distance, and by  $2.2^\circ$  in absolute longitudinal distance. The average simulation time did not differ (with an accuracy of 1%) from that of the non-degraded model with  $2,000 \text{ particles mm}^{-1} \text{ h}^{-1}$ . The output from 'hpa100' differed from that of the baseline model by an average of ten percentage points in CRR, by  $2.2^\circ$  in absolute latitudinal distance, and by  $3.3^\circ$  in absolute longitudinal distance. The average simulation time was 1% higher than that of the non-degraded model. The output from 'hpa200' differed from that of the baseline model by an average of 17 percentage points in CRR, by  $3.7^\circ$  in absolute latitudinal distance, and by  $4.8^\circ$  in absolute longitudinal distance. The average simulation time was 5% higher than that of the non-degraded model. The output from '5k25' differed from that of the baseline model by an average of one percentage point in CRR, by  $0.6^\circ$  in absolute latitudinal distance, and by  $0.6^\circ$  in absolute longitudinal distance. The average simulation time was 4% lower than that of the non-degraded model. The output from '5k50' differed from that of the baseline model by an average of four percentage points in CRR, by  $1.0^\circ$  in absolute latitudinal distance, and by  $1.3^\circ$  in absolute longitudinal distance. The average simulation time was 1% lower than that of the non-degraded model. Finally, the output from '5k100' differed from



that of the baseline model by an average of nine percentage points in CRR, by  $2.4^\circ$  in absolute latitudinal distance, and by  $3.1^\circ$   
315 in absolute longitudinal distance. The average simulation time did not differ from that of the non-degraded model.

The effects of adjustments to the vertical profile can also be seen from the evaporation footprints from Manaus, with larger flows southward and eastward (Fig. 7), and from the other locations (Figs. S26–S31).

### 3.6 Effect of time steps

320 We find a low sensitivity of the footprints to time step  $dt$ . For  $dt = 0.01$  h and  $dt = 0.05$  h, we find no difference in CRR, absolute latitudinal distance or absolute longitudinal distance with the baseline model, which has  $dt = 0.1$  h. For  $dt = 0.5$  h and  $dt = 1$  h, we find no difference in CRR, but we do find a small difference of  $0.1^\circ$  in mean absolute longitudinal distance and mean absolute latitudinal difference with the baseline model. The low sensitivity to the chosen time step is confirmed by the practically indistinguishable footprints (Figs. 8. S32–S37).

325

The runs with  $dt = 0.01$  h were nine times slower than those with  $dt = 0.1$  h. The ones with  $dt = 0.05$  were two times slower, the ones with  $dt = 0.5$  h were four times faster, and the ones with  $dt = 1$  h were seven times faster.

### 3.7 Effects of vertical mixing probabilities

Because the rate of vertical mixing in the atmosphere is unknown, there can be no baseline model to compare results against.  
330 However, we tested the sensitivity of downwind evaporation footprint to eight different rates of vertical mixing. These eight rates consist of those with and without accounting for large-scale vertical flow in the ERA5 reanalysis data (called ‘omega’) and of four different randomized mixing probabilities: that at which full vertical mixing takes place on average every hour, every six hours, every 24 hours and every 120 hours.

335 In the simulations in which we did not account for omega, CRR decreased slightly with average mixing time (i.e. with lower mixing probability): averaged across the source locations, CRR decreases by one percentage point at each stepwise decrease in mixing probability, i.e. from hourly to six-hourly mixing, from six-hourly mixing to daily mixing, and from daily mixing to 120-hourly mixing. The absolute latitudinal transport distance increased from hourly to six-hourly mixing by an average of  $0.7^\circ$ . From six-hourly mixing to 24-hourly mixing this increased by another  $0.2^\circ$ , but from 24-hourly to 120-hourly mixing it  
340 decreased by  $0.3^\circ$ . The absolute longitudinal transport distance increased from hourly to six-hourly mixing by an average of  $0.5^\circ$ , increased from six-hourly mixing to 24-hourly mixing by  $0.1^\circ$ , and decreased from 24-hourly mixing to 120-hourly mixing by  $0.5^\circ$ . The larger spread of rainfall locations from the point sources is also clearly visible from the footprints (Figs. 9, S38–S43).



345 In the simulations in which we did account for omega, CRR decreased much more rapidly mixing time than in the simulations  
without omega: from one-hourly to six-hourly mixing, mean CRR decreased by ten percentage points, from six-hourly to daily  
mixing it decreased by nine percentage points, and from daily to 120-hourly mixing by four percentage points. The absolute  
latitudinal transport distance increased monotonically with mixing time: from hourly to six-hourly mixing by an average of  
2.1°, from six-hourly to daily mixing by 0.6°, and from daily to 120-hourly mixing by 0.1°. The absolute longitudinal transport  
350 distance increased from hourly to six-hourly mixing by an average of 2.3°, increased from six-hourly mixing to 24-hourly  
mixing by 0.8°, and increased from 24-hourly mixing to 120-hourly mixing by 0.4°. Also here, the figures show that slower  
vertical mixing increases the area where rainfall depends on evaporation from the studied sources. However, with omega, the  
rainfall from the sources is more equally distributed within the footprints than without omega. In other words, with omega the  
footprints show a pattern that is less influenced by diffusion (Figs. 9, S38–S43).

355  
CRR was higher without omega than with omega, a difference that increased with mixing time. At hourly mixing, the mean  
difference was four percentage points, at six-hourly mixing 13 percentage points, at daily mixing 21 percentage points, and at  
120-hourly mixing 25 percentage points. Absolute latitudinal transport distance was higher with omega than without omega,  
and also this difference increased with mixing time: at hourly mixing, the mean difference was 1.1°, at six-hourly mixing 2.5°,  
360 at daily mixing 2.9°, and at 120-hourly mixing 3.3°. Similarly, absolute longitudinal transport distance was consistently higher  
with omega than without omega: at hourly mixing, the mean difference was 1.5°, at six-hourly mixing 3.3°, at daily mixing  
3.9°, and at 120-hourly mixing 4.8°.

When omega was not accounted for, the simulations ran consistently faster with larger mixing times: from hourly to six-hourly  
365 mixing by 7%, from six-hourly to daily mixing by 4%, and from daily to 120-hourly mixing by 3%. With omega included, the  
simulation times did not show a pattern: from hourly to six-hourly mixing it decreased by 2%, but from six-hourly to daily  
mixing it increased by 2%, and from daily to 120-hourly mixing it increased by another 1%. Averaged across all simulations,  
the calculations without omega ran 11% faster than those with omega.

#### 4 Discussion

370 Our aim was to identify an optimal model to track the global flows of atmospheric moisture accurately and efficiently given  
the best available data. Therefore, we tested how different types of moisture tracking models and their assumptions, forced  
with the high-resolution ERA5 reanalysis data, produced different ‘footprints’ of evaporation from source locations. Below,  
we evaluate our results and use them to propose such an optimal model for which we publish the code.

375 We first tested the performance of the two main classes of moisture tracking models, Eulerian and Lagrangian, implemented  
in two and three spatial dimensions. Eulerian models are grid-based, meaning that at each time step moisture is exchanged



between neighbouring grid cells. Lagrangian models track moisture particles in continuous space, meaning that at each time step the coordinates of the particles are updated. In both cases, the moisture budget is also updated at each time step based on the local precipitation, evaporation and precipitable water. Under the premise that tracking moisture flows becomes more accurate by processing more detailed atmospheric information, we compared our results to a three-dimensional Lagrangian that is based on as much information as possible and tracks the very large amount of  $10,000 \text{ particles mm}^{-1} \text{ evaporation h}^{-1}$ . For both the Eulerian models and the two-dimensional Lagrangian model, we found large errors ( $>10$  percentage points) in the hydrologically important variable of continental evaporation recycling ratio (CRR), which is the proportion of evaporated moisture that precipitates on land. Also the distances of moisture transport differed by several degrees for each of these models. For many purposes, such errors are too large, while no benefit was reached regarding simulation time: both the two- and three-dimensional Eulerian models were considerably slower (58 and 73 times) than their Lagrangian equivalents. Thus, for point sources, it can be concluded that Eulerian models, on the resolution of the ERA5 data, are not efficient compared to Lagrangian models. Although a two-dimensional Lagrangian model is fastest, the errors that result from the simplification from three to two dimensions will generally be considered too large. Therefore, we argue that an optimal moisture tracking model using ERA5 data should be a three-dimensional Lagrangian one.

We found that the accuracy of the output of the Lagrangian model was not very sensitive to the amount of particles that were tracked for each mm of evaporation per hour, while much simulation time can be saved by minimising that amount. At  $500 \text{ particles mm}^{-1} \text{ h}^{-1}$ , the model performance was always as good as when more particles were tracked, so we conclude that this is a sufficiently large amount of particles to track from point sources for one month. When the moisture is tracked from an area rather than a source, or when a longer study period is concerned, it may be justified to track even fewer particles. This is especially the case when one is interested in mean moisture flows rather than highly detailed spatial or temporal differences. The reason is that when a larger amount of evaporation is being considered (i.e. due to an expansion of study area or period), the total amount of particles that is tracked can be kept equal with a corresponding reduction of amount of particles  $\text{mm}^{-1} \text{ h}^{-1}$ .

The effect of the height in the atmospheric column at which moisture was released at the start of the simulation resulted in small but measurable differences in the distance of the flows, where moisture release according to the vertical moisture profile yielded longer distances than moisture release at the surface. However, eventually, which model is most suitable depends on the aim of the simulation. Generally, one would want to track evaporation rather than already-present atmospheric moisture. Because evaporation occurs at the surface, and following a similar assessment by Van der Ent et al. (2013), surface release will be the default in our model.

The level of detail of the atmospheric moisture profile matters. We found that especially the degradation of this information introduced significant errors, so we advise against doing that. In addition, interpolation of the ERA5 reanalysis data (in three spatial dimensions and the temporal dimension) affected the footprints of evaporation, while its effect on simulation time was



marginal. Therefore, we conclude that, even when all available atmospheric layers in ERA5 are used, interpolating the data is still advisable, as did previous studies using Lagrangian models (Tuinenburg et al., 2012, 2014; Van der Ent et al., 2013; Van der Ent and Tuinenburg, 2017; Tuinenburg and van der Ent, 2019).

415 The time steps for calculation ( $dt$ ) that we evaluated had little effect on the evaporation footprints and their statistics, but did affect the simulation times significantly. A value of  $dt = 0.1$  h, the time step chosen in the baseline model, gave the same results as smaller values of  $dt$ , while increasing it above that did introduce some errors. Therefore,  $dt = 0.1$  h seems optimal.

We tested the effects of eight different assumptions on the speed of mixing in the vertical direction. In this case there is no ideal (baseline) model to compare results against, because the real vertical mixing speed in the atmosphere is unknown, leaving only a relative comparison. Atmospheric reanalysis data do include vertical wind speeds ('omega'), but these are only grid-scale flows and do not include turbulence and convection, which have a large influence on the vertical mixing. However, while it is known that omega underestimates vertical mixing, the extent to which it does is not. Therefore, moisture tracking models may disregard omega and either choose another method to account for vertical mixing, such as based on turbulent mixing (Stohl et al., 2005), transporting particles on isentropic levels (Dirmeyer and Brubaker, 2007), or distribute the moisture budget errors over the vertical layers (WAM-2layers; Van der Ent et al., 2014). In our case, at each time step each moisture particle had a certain probability of being relocated within the atmospheric column (randomly, but scaled with the humidity content of the atmosphere). These probabilities were chosen such that on average every hour, six hours, 24 hours or 120 hours full mixing will have occurred. All four options were assessed with and without additionally accounting for large scale vertical wind speed.

420  
425  
430 We found that whether or not omega was accounted for had a large effect on the results. This is to be expected especially when many vertical layers are used between which flows take place. The effect of omega declines with more rapid randomized mixing. Because of the uncertainties related to vertical mixing, we leave the mixing time and inclusion of omega as an option in the model. As default we take a mixing time of 24 h without omega. The rationale for choosing 24 h is twofold: first, it is within the range (6–24 h) where the results are relatively robust to the choice of mixing time; second, atmospheric mixing follows a diurnal cycle (Tuinenburg and van der Ent, 2019), which is averaged out by mixing continuously with a full mixing every 24 hours. We assume that this speed of mixing is rapid enough to supersede larger-scale vertical flows so as to simplify the model and exclude omega.

435  
440

The uncertainty regarding the process of vertical mixing combined with the sensitivity of moisture recycling to the vertical mixing introduces a corresponding uncertainty in any moisture recycling result. Based on our sensitivity analysis, it can be expected that in this respect alone, the uncertainty in transport distance is limited to several tens of degrees in both latitudinal and longitudinal directions. Continental recycling ratio differed only by a few percentage points depending on mixing assumptions. In case randomized mixing, representing turbulence, would need to be complemented by omega, the uncertainty becomes very sensitive to the level of turbulence. We found that continental recycling ratios could differ in the range of ten



445 percentage points and transport distances by several degrees. These are large uncertainties, so we argue that a better constraint  
of vertical mixing could greatly improve the accuracy of moisture tracking models in the future.

We used a selection of point sources and tracked the destinations of their evaporation for a single arbitrary month (July 2012).  
Although moisture recycling can strongly vary both spatially and temporally (Brubaker et al., 1993; Gimeno et al., 2012), we  
450 chose to focus on the spatial variation to cover a range of terrains, latitudes, and wind patterns, as the effects of different model  
assumptions may become apparent by studying different regions especially (Goessling and Reick, 2013). The purpose here  
was to compare the performance of different models and their assumptions for a range of hydrological statistics as well as  
simulation time. Thus, the footprints may differ in their representativeness for the respective locations, but they are helpful in  
visualising the consequences of different assumptions in atmospheric moisture tracking.

455 Many moisture recycling studies have used low-spatial-resolution Eulerian models (typically  $1.5^\circ$  with one or two vertical  
layers) forced with ERA-Interim reanalysis data (Dee et al., 2011). When Eulerian models are run on coarse spatial scales, the  
risk of numerical instability due to large Courant numbers is contained. However, we advise to be cautious when developing  
Eulerian models based on the resolution of ERA5 data, because of the large moisture fluxes compared to the grid cell size and  
460 the numerical dispersion when this is mitigated by using smaller time steps. Downgrading the data to coarser resolutions such  
as  $1.5^\circ$  would circumvent the problem, but comes at the cost of large losses of information. The Lagrangian model we present  
here does not suffer from numerical issues caused by a grid-based approach, and can be expected to become more accurate  
with the availability of more accurate atmospheric data.

465 The fact that the errors in moisture recycling estimates depended on the study area means that one should be cautious with  
generalizing the implications of these outcomes. An example of moisture flow above complex terrain is the evaporation from  
Manaus in the Amazon, where westward moisture flows are blocked by the Andes and partially diverted southward, but also  
partially pass over the mountain range and precipitate over the Pacific Ocean. We argue that for areas with relatively complex  
terrain in particular, three-dimensional Lagrangian models are most suitable because these describe atmospheric moisture  
470 transport better under situations with strong vertical variability in horizontal moisture transport.

## 5 Conclusions

Moisture recycling science has a long history, with gradually improved models depending on the state-of-the-art data, from  
early one-dimensional work to explicit moisture tracking in two-dimensional and three-dimensional Eulerian and Lagrangian  
models. This model development has gone hand-in-hand with improved data development. With the development of the new  
475 ERA5 reanalysis data, data limitations have reduced considerably. We evaluated the performance of different model types  
given these new data. Our comprehensive sensitivity analysis led us to propose an optimal three-dimensional Lagrangian



moisture tracking model – one that is able to produce highly detailed ‘footprints’ of evaporation and that is devoid of unnecessary complexity. It therefore runs relatively fast with negligible loss of information. We make the code for this model freely available.

#### 480 **Code and data availability**

The model code is available at: <https://github.com/ObbeTuinenburg/U-Track>. The ERA5 data are available at: <https://cds.climate.copernicus.eu/cdsapp#!/home>.

#### **Author contribution**

OAT conceived and designed the study. Both authors carried out the study, interpreted the results and wrote the paper.

#### 485 **Acknowledgments**

We thank Ruud van der Ent, Ingo Fetzer, Line Gordon and Lan Wang-Erlandsson for useful discussions. We thank the Bolin Centre for Climate Research for funding the stay of OAT at the Stockholm Resilience Centre. OAT acknowledges support from the research program Innovational Research Incentives Scheme Veni (016.veni.171.019), funded by the Netherlands Organisation for Scientific Research (NWO). AS acknowledges support from the European Research Council project Earth  
490 Resilience in the Anthropocene (743080 ERA).

#### **References**

- Bosilovich, M. G.: On the vertical distribution of local and remote sources of water for precipitation, *Meteorology and Atmospheric Physics*, 80(1), 31–41, doi:10.1007/s007030200012, 2002.
- 495 Brubaker, K. L., Entekhabi, D. and Eagleson, P. S.: Estimation of continental precipitation recycling, *Journal of Climate*, 6(6), 1077–1089, doi:10.1175/1520-0442(1993)006<1077:EOCPR>2.0.CO;2, 1993.
- Burde, G. I. and Zangvil, A.: The estimation of regional precipitation recycling. Part I: review of recycling models, *J. Climate*, 14(12), 2497–2508, doi:10.1175/1520-0442(2001)014<2497:TEORPR>2.0.CO;2, 2001.
- Copernicus Climate Change Service (C3S): ERA5: Fifth generation of ECMWF atmospheric reanalyses of the global climate, Copernicus Climate Change Service Climate Data Store (CDS), doi:<https://cds.climate.copernicus.eu/cdsapp#!/home>, n.d.
- 500 Dee, D. P., Uppala, S. M., Simmons, A. J., Berrisford, P., Poli, P., Kobayashi, S., Andrae, U., Balmaseda, M. A., Balsamo, G. and Bauer, P.: The ERA- Interim reanalysis: configuration and performance of the data assimilation system, *Quarterly Journal of the Royal Meteorological Society*, 137(656), 553–597, doi:10.1002/qj.828, 2011.





- Dirmeyer, P. A. and Brubaker, K. L.: Characterization of the global hydrologic cycle from a back-trajectory analysis of atmospheric water vapor, *Journal of Hydrometeorology*, 8(1), 20–37, doi:10.1175/JHM557.1, 2007.
- 505 Dominguez, F., Kumar, P., Liang, X.-Z. and Ting, M.: Impact of atmospheric moisture storage on precipitation recycling, *Journal of Climate*, 19(8), 1513–1530, doi:10.1175/JCLI3691.1, 2006.
- Gimeno, L., Stohl, A., Trigo, R. M., Dominguez, F., Yoshimura, K., Yu, L., Drumond, A., Durán-Quesada, A. M. and Nieto, R.: Oceanic and terrestrial sources of continental precipitation, *Reviews of Geophysics*, 50(4), doi:10.1029/2012RG000389, 2012.
- 510 Goessling, H. F. and Reick, C. H.: What do moisture recycling estimates tell us? Exploring the extreme case of non-evaporating continents, *Hydrology and Earth System Sciences*, 15, 3217–3235, 2011.
- Goessling, H. F. and Reick, C. H.: On the “well-mixed” assumption and numerical 2-D tracing of atmospheric moisture, *Atmospheric Chemistry and Physics*, 13, 5567–5585, doi:10.5194/acp-13-5567-2013, 2013.
- 515 Keys, P. W., Wang-Erlandsson, L. and Gordon, L. J.: Revealing invisible water: moisture recycling as an ecosystem service, *PloS ONE*, 11(3), e0151993, doi:10.1371/journal.pone.0151993, 2016.
- Keys, P. W., Wang-Erlandsson, L. and Gordon, L. J.: Megacity precipitation sheds reveal tele-connected water security challenges, *PloS one*, 13(3), e0194311, doi:10.1371/journal.pone.0194311, 2018.
- Singh, H. A., Bitz, C. M., Nusbaumer, J. and Noone, D. C.: A mathematical framework for analysis of water tracers: Part 1: Development of theory and application to the preindustrial mean state, *Journal of Advances in Modeling Earth Systems*, 8(2), 991–1013, doi:10.1002/2016MS000649, 2016.
- 520 Spracklen, D. V., Baker, J. C. A., Garcia-Carreras, L. and Marsham, J.: The effects of tropical vegetation on rainfall, *Annual Review of Environment and Resources*, 43(1), 193–218, doi:10.1146/annurev-environ-102017-030136, 2018.
- Staal, A., Tuinenburg, O. A., Bosmans, J. H. C., Holmgren, M., van Nes, E. H., Scheffer, M., Zemp, D. C. and Dekker, S. C.: Forest-rainfall cascades buffer against drought across the Amazon, *Nature Climate Change*, 8(6), 539–543, doi:10.1038/s41558-018-0177-y, 2018.
- 525 Stohl, A., Forster, C., Frank, A., Seibert, P. and Wotawa, G.: The Lagrangian particle dispersion model FLEXPART version 6.2, *Atmospheric Chemistry and Physics*, 5(9), 2461–2474, doi:10.5194/acp-5-2461-2005, 2005.
- Tuinenburg, O. A. and van der Ent, R. J.: Land surface processes create patterns in atmospheric residence time of water, *Journal of Geophysical Research: Atmospheres*, 124(2), 583–600, doi:10.1029/2018JD028871, 2019.
- 530 Tuinenburg, O. A., Hutjes, R. W. A. and Kabat, P.: The fate of evaporated water from the Ganges basin, *Journal of Geophysical Research: Atmospheres*, 117(D1), D01107, doi:10.1029/2011JD016221, 2012.
- Tuinenburg, O. A., Hutjes, R. W. A., Stacke, T., Wiltshire, A. and Lucas-Picher, P.: Effects of irrigation in India on the atmospheric water budget, *Journal of Hydrometeorology*, 15(3), 1028–1050, doi:10.1175/JHM-D-13-078.1, 2014.
- 535 Van der Ent, R. J. and Savenije, H. H. G.: Length and time scales of atmospheric moisture recycling, *Atmospheric Chemistry and Physics*, 11(5), 1853–1863, doi:10.5194/acp-11-1853-2011, 2011.
- Van der Ent, R. J. and Tuinenburg, O. A.: The residence time of water in the atmosphere revisited, *Hydrology and Earth System Sciences*, 21(2), 779–790, doi:10.5194/hess-21-779-2017, 2017, 2017.



- Van der Ent, R. J., Savenije, H. H. G., Schaefli, B. and Steele-Dunne, S. C.: Origin and fate of atmospheric moisture over continents, *Water Resources Research*, 46, W09525, doi:10.1029/2010WR009127, 2010.
- 540 Van der Ent, R. J., Tuinenburg, O. A., Knoche, H. R., Kunstmann, H. and Savenije, H. H. G.: Should we use a simple or complex model for moisture recycling and atmospheric moisture tracking?, *Hydrology and Earth System Sciences*, 17(12), 4869–4884, doi:10.5194/hess-17-4869-2013, 2013.
- Van der Ent, R. J., Wang-Erlandsson, L., Keys, P. W. and Savenije, H. H. G.: Contrasting roles of interception and transpiration in the hydrological cycle-Part 2: Moisture recycling, *Earth System Dynamics*, 5(2), 471–489, 2014.
- 545 Wang-Erlandsson, L., Fetzer, I., Keys, P. W., van der Ent, R. J., Savenije, H. H. G. and Gordon, L. J.: Remote land use impacts on river flows through atmospheric teleconnections, *Hydrology and Earth System Sciences*, 22(8), 4311–4328, doi:10.5194/hess-22-4311-2018, 2018.
- Yoshimura, K., Oki, T., Ohte, N. and Kanae, S.: Colored moisture analysis estimates of variations in 1998 Asian monsoon water sources, *Journal of the Meteorological Society of Japan. Ser. II*, 82(5), 1315–1329, doi:10.2151/jmsj.2004.1315, 2004.
- 550 Zemp, D. C., Schleussner, C. F., Barbosa, H. M. J., van der Ent, R. J., Donges, J. F., Heinke, J., Sampaio, G. and Rammig, A.: On the importance of cascading moisture recycling in South America, *Atmospheric Chemistry and Physics*, 14(23), 13337–13359, doi:10.5194/acp-14-13337-2014, 2014.
- Zemp, D. C., Schleussner, C. F., Barbosa, H. M. J., Hirota, M., Montade, V., Sampaio, G., Staal, A., Wang-Erlandsson, L. and Rammig, A.: Self-amplified Amazon forest loss due to vegetation-atmosphere feedbacks, *Nature Communications*, 8, 14681, doi:10.1038/ncomms14681, 2017.
- 555



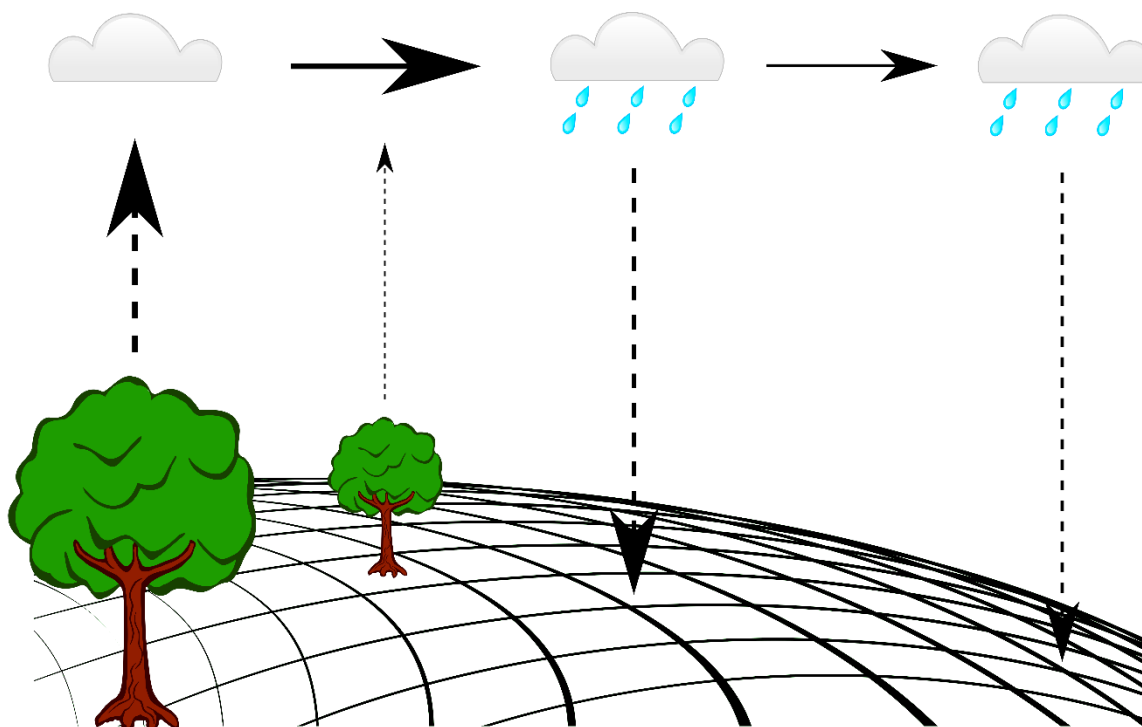
## Tables and Figures

560 **Table 1: Continental recycling ratio (%), absolute latitudinal distance (°), absolute longitudinal distance (°), mean latitudinal change (°), mean longitudinal change (°), and calculation time (CPU seconds) for the baseline, two-dimensional Eulerian, three-dimensional Eulerian, two-dimensional Lagrangian, and three-dimensional Lagrangian model versions for each of the seven point sources considered in July 2012.**

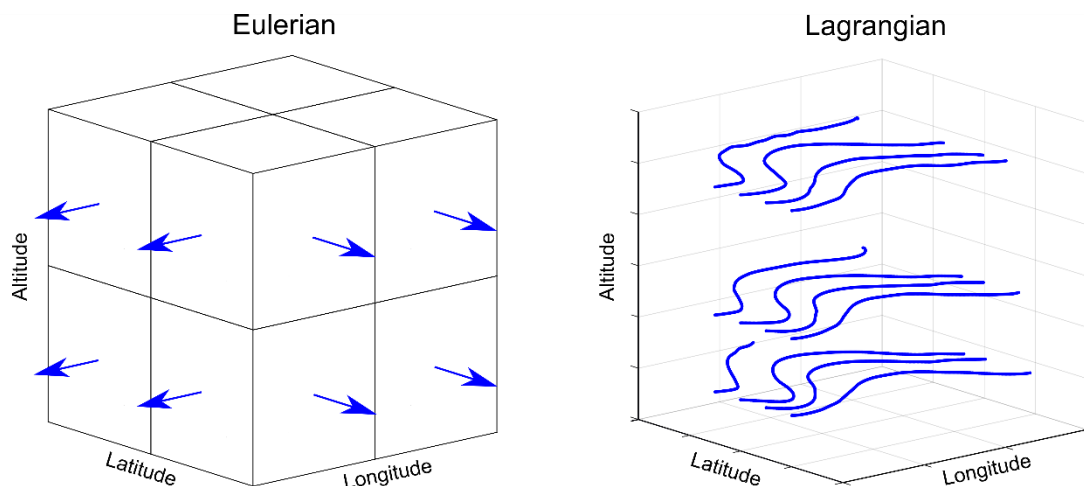
	Baseline	2D Eulerian	3D Eulerian	2D Lagrangian	3D Lagrangian
Continental recycling ratio (%)					
Chendu	94	99	96	72	94
Kansas	44	51	47	38	44
Manaus	68	91	76	38	68
Nagpur	94	78	80	77	94
Nairobi	87	73	62	75	87
Stockholm	63	83	80	51	63
Utrecht	45	35	34	42	44
Absolute latitudinal distance (°)					
Chendu	2.6	1.1	1.0	5.8	2.6
Kansas	7.2	1.7	2.8	7.6	7.2
Manaus	4.8	0.8	1.4	6.6	4.8
Nagpur	5.1	1.7	1.2	5.9	5.1
Nairobi	7.3	4.0	2.3	14.8	7.3
Stockholm	7.4	2.6	2.5	8.1	7.5
Utrecht	11.4	2.9	3.1	12.4	11.5
Absolute longitudinal distance (°)					
Chendu	3.4	0.8	1.7	6.2	3.4
Kansas	19.6	9.2	9.3	20.6	19.6
Manaus	15.0	8.6	7.5	14.3	15.0
Nagpur	5.1	5.7	4.3	6.6	5.1
Nairobi	6.1	1.9	2.4	11.0	6.1
Stockholm	15.0	7.0	6.0	16.8	15.1
Utrecht	16.0	13.7	11.7	18.2	16.0
Mean latitudinal change (°)					
Chendu	2.3	0.6	0.1	5.6	2.3



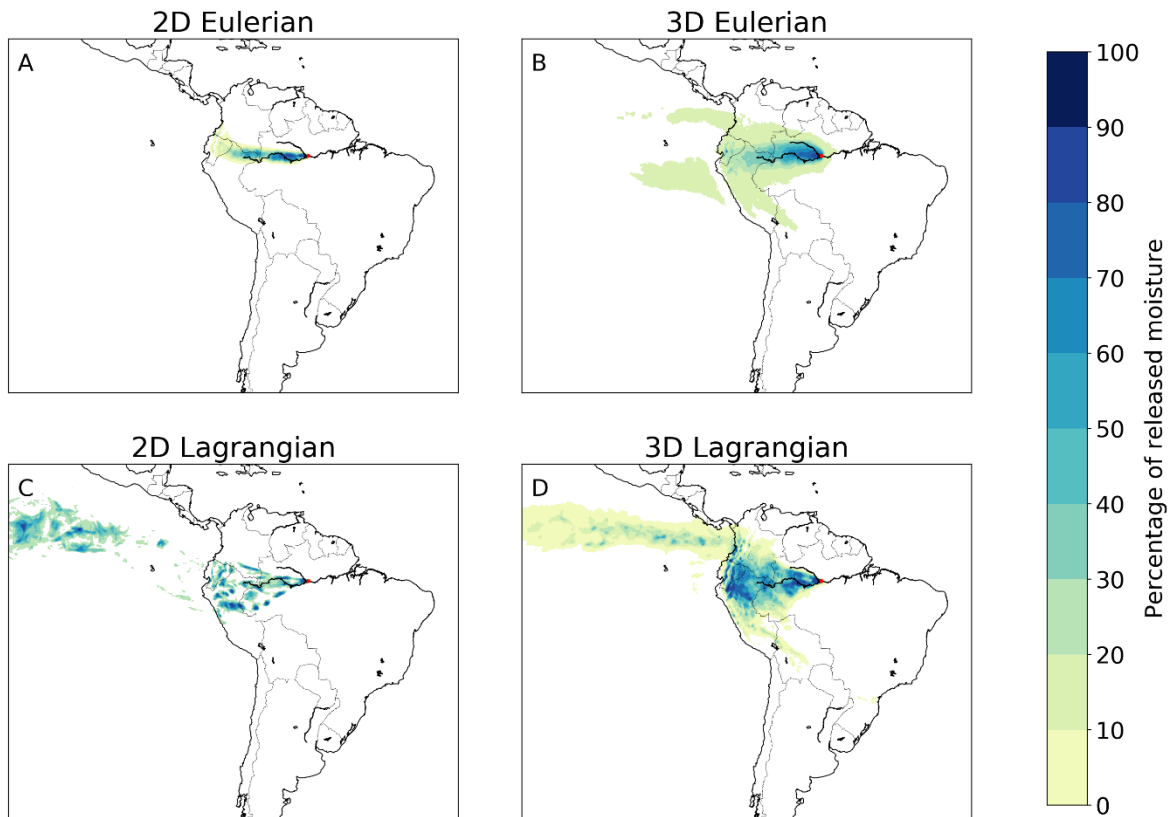
Kansas	4.0	1.3	1.8	4.5	4.0
Manaus	1.5	0.4	0.0	4.3	1.5
Nagpur	4.9	1.3	1.3	5.8	4.9
Nairobi	7.2	4.0	2.2	14.8	7.2
Stockholm	1.3	2.6	2.3	0.0	1.3
Utrecht	6.1	2.8	3.1	8.5	6.0
Mean longitudinal change (°)					
Chendu	2.4	0.6	0.9	6.0	2.4
Kansas	15.2	9.2	8.5	14.6	15.2
Manaus	-14.3	-8.6	-7.4	-14.3	-14.4
Nagpur	3.6	5.7	3.8	5.2	3.6
Nairobi	3.0	-1.6	0.8	6.2	3.0
Stockholm	11.1	-0.6	-1.4	13.3	11.1
Utrecht	15.3	11.3	9.8	17.9	15.4
Calculation time (CPU seconds)					
Chendu	821	2612	20366	35	166
Kansas	2182	2601	20229	69	439
Manaus	1553	2670	21713	53	313
Nagpur	808	2655	20275	25	163
Nairobi	924	2663	20733	31	186
Stockholm	1623	2611	20140	52	327
Utrecht	1774	2741	19836	57	357



570 **Figure 1: Moisture tracking from source to sink. All moisture tracking models use atmospheric reanalysis data to simulate the locations of moisture. At each time step, moisture budgets are updated based on wind speed and directions (horizontal arrows), evaporation (dashed arrows up) and precipitation (dashed arrows down). This leads to source-to-sink estimates of atmospheric moisture flows, such as the evaporation footprints and basin recycling ratios in this study.**



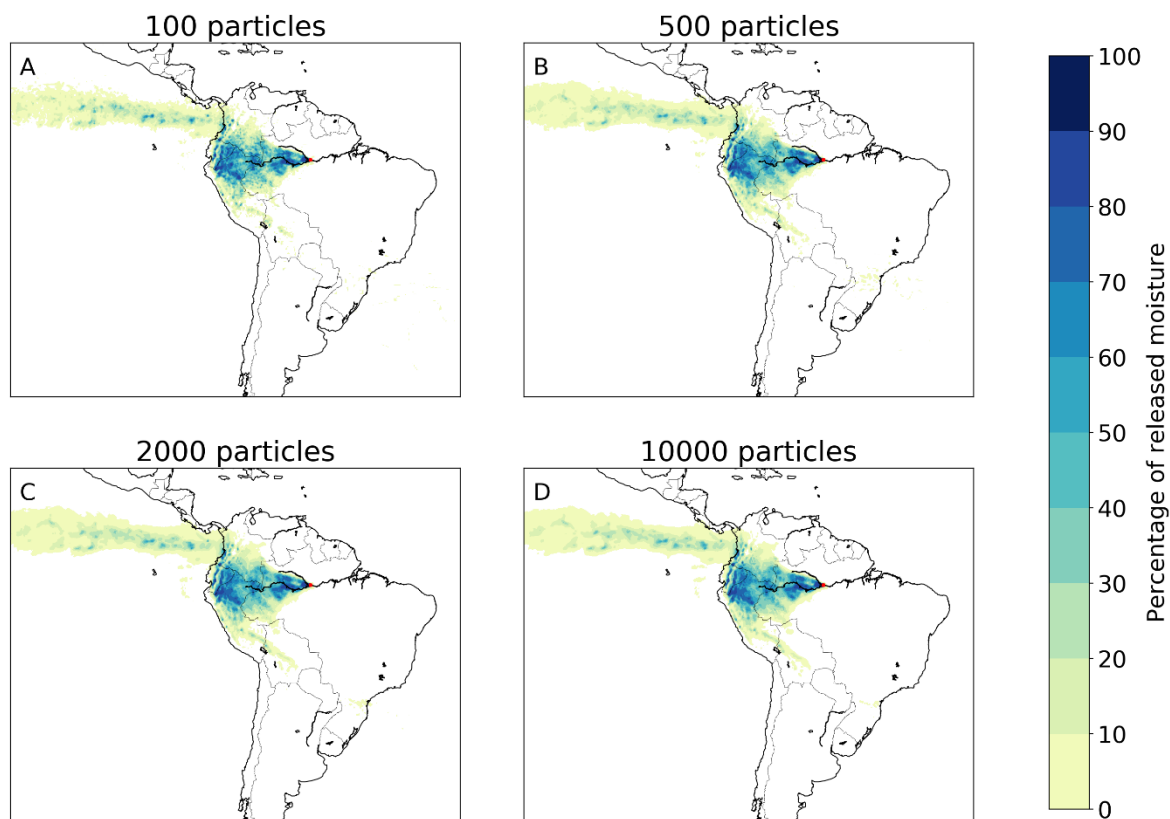
575 **Figure 2: The difference between Eulerian and Lagrangian moisture tracking models. A) Eulerian models are grid-based, meaning that the study area is divided into a two- or three-dimensional grid of cells. At each time step, the tracked moisture content of each grid cell is updated based on estimated cell-to-cell winds, precipitation, and evaporation. B) Lagrangian models are trajectory-based, meaning that a number of moisture parcels have coordinates. At each time step, the coordinates and the tracked moisture content of the parcels are updated based on point-based wind flows, precipitation, and evaporation.**



580

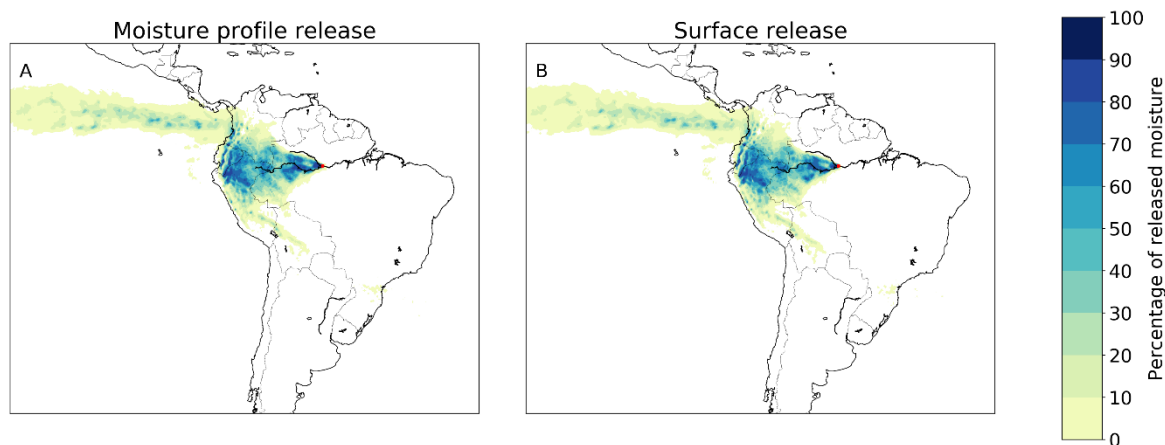
**Figure 3: Different footprints of moisture releases from Manaus in July 2012 in two-dimensional and three-dimensional Eulerian and Lagrangian models. A) Two-dimensional Eulerian, with a mean latitudinal moisture flow of  $0.4^\circ$  in northerly direction and mean longitudinal flow of  $8.6^\circ$  in westerly direction; B) Three-dimensional Eulerian, with a mean latitudinal moisture flow of  $0.0^\circ$  in northerly/southerly direction and mean longitudinal flow of  $7.4^\circ$  in westerly direction; C) Two-dimensional Lagrangian, with a mean latitudinal moisture flow of  $4.3^\circ$  in northerly direction and mean longitudinal flow of  $14.3^\circ$  in westerly direction; D) Three-dimensional Lagrangian, with a mean latitudinal moisture flow of  $1.5^\circ$  in northerly direction and mean longitudinal flow of  $14.4^\circ$  in westerly direction.**

585

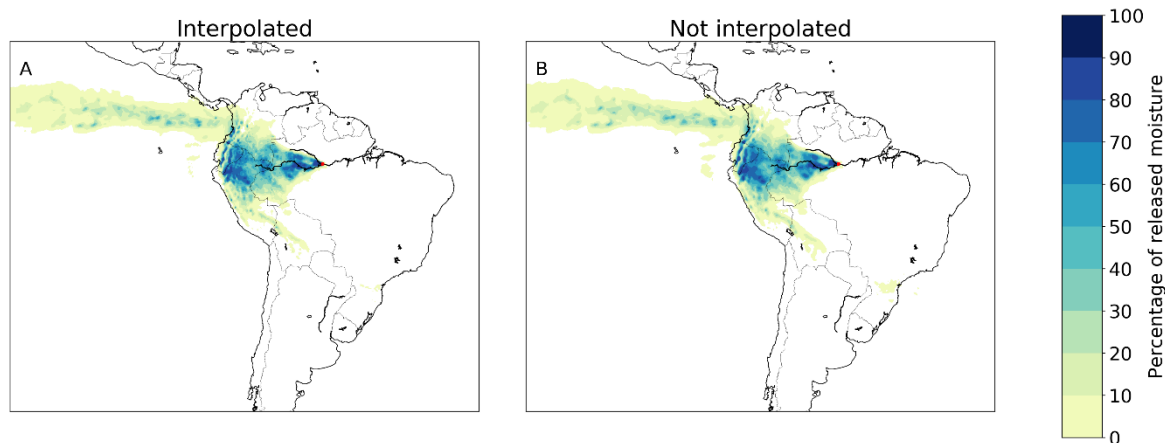


590 **Figure 4: Different footprints of moisture releases from Manaus in July 2012 in a three-dimensional Lagrangian model**  
**with 100, 500, 2,000, and 10,000 tracked particles  $\text{mm}^{-1} \text{h}^{-1}$ ).** A) 100 particles, with a mean latitudinal moisture flow of  
 **$1.4^\circ$  in northerly direction and mean longitudinal flow of  $14.2^\circ$  in westerly direction;** B) 500 particles, with a mean  
latitudinal moisture flow of  $1.4^\circ$  in northerly direction and mean longitudinal flow of  $14.3^\circ$  in westerly direction; C)  
2,000 particles, with a mean latitudinal moisture flow of  $1.5^\circ$  in northerly direction and mean longitudinal flow of  $14.4^\circ$   
595 in westerly direction; D) 10,000 particles, with a mean latitudinal moisture flow of  $1.5^\circ$  in northerly direction and mean  
longitudinal flow of  $14.3^\circ$  in westerly direction.





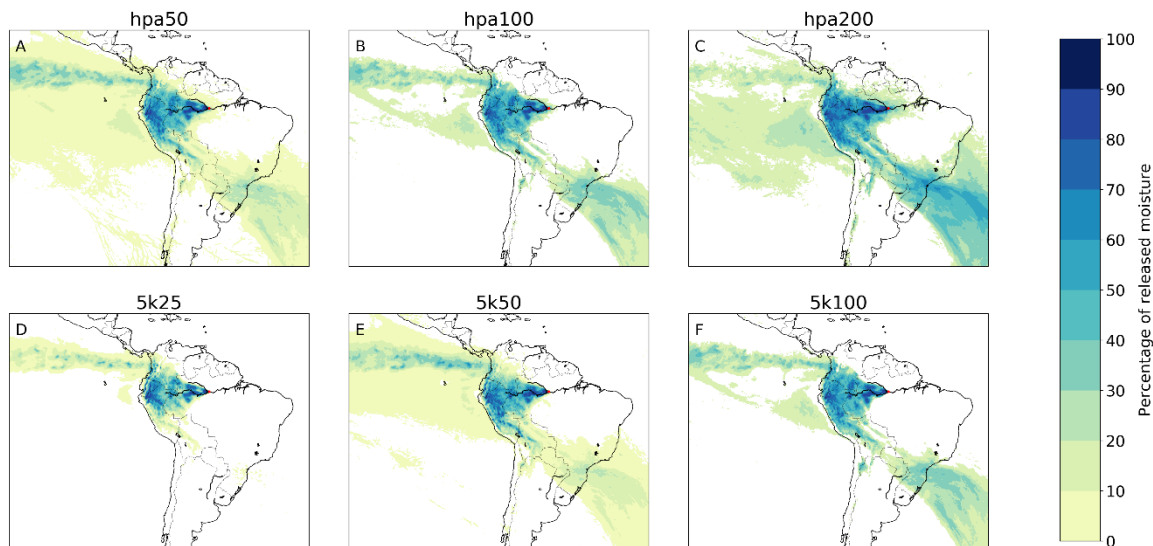
600 **Figure 5: Different footprints of moisture releases from Manaus in July 2012 in a three-dimensional Lagrangian model with moisture released according to the vertical moisture profile of the atmosphere and moisture released at the surface. A) Release according to the moisture profile, with a mean latitudinal moisture flow of  $1.5^\circ$  in northerly direction and mean longitudinal flow of  $14.4^\circ$  in westerly direction; B) Release at the surface, with a mean latitudinal moisture flow of  $1.3^\circ$  in northerly direction and mean longitudinal flow of  $14.2^\circ$  in westerly direction.**



605 **Figure 6: Different footprints of moisture releases from Manaus in July 2012 in a three-dimensional Lagrangian model with and without interpolation of wind speed and directions. A) Interpolated, with a mean latitudinal moisture flow of  $1.5^\circ$  in northerly direction and mean longitudinal flow of  $14.4^\circ$  in westerly direction; B) Not interpolated, with a mean latitudinal moisture flow of  $1.4^\circ$  in northerly direction and mean longitudinal flow of  $14.3^\circ$  in westerly direction.**



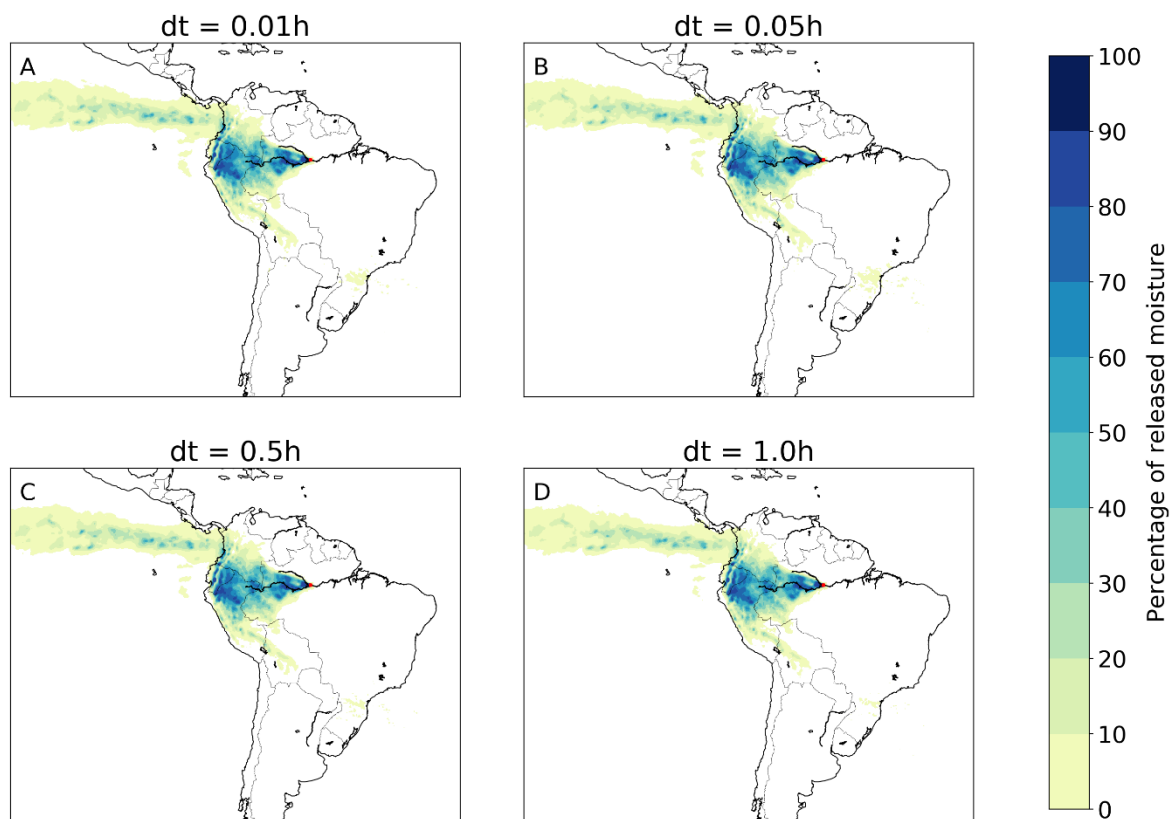
610



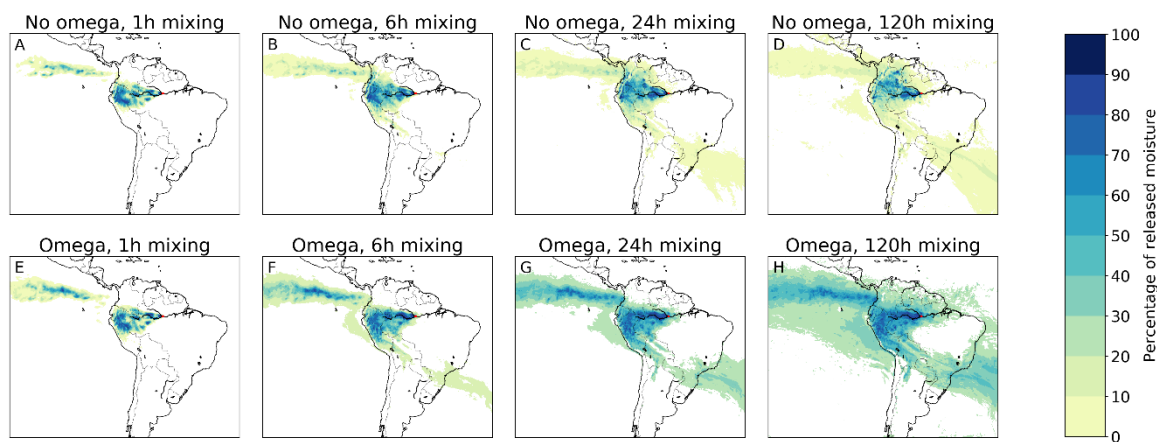
615

**Figure 7: Different footprints of moisture releases from Manaus in July 2012 in a three-dimensional Lagrangian model with different degradations of the vertical moisture profile. A) hpa50, with a mean latitudinal moisture flow of  $2.8^\circ$  in southerly direction and mean longitudinal flow of  $11.0^\circ$  in westerly direction; B) hpa100, with a mean latitudinal moisture flow of  $5.3^\circ$  in southerly direction and mean longitudinal flow of  $9.2^\circ$  in westerly direction; C) hpa200, with a mean latitudinal moisture flow of  $17.6^\circ$  in southerly direction and mean longitudinal flow of  $1.8^\circ$  in westerly direction; D) 5k25, with a mean latitudinal moisture flow of  $1.7^\circ$  in northerly direction and mean longitudinal flow of  $14.4^\circ$  in westerly direction; E) 5k50, with a mean latitudinal moisture flow of  $2.8^\circ$  in southerly direction and mean longitudinal flow of  $11.6^\circ$  in westerly direction; F) 5k100, with a mean latitudinal moisture flow of  $5.1^\circ$  in southerly direction and mean longitudinal flow of  $9.6^\circ$  in westerly direction.**

620



625 **Figure 8: Different footprints of moisture releases from Manaus in July 2012 in a three-dimensional Lagrangian model with different time steps ( $dt$ ): 0.01 hours, 0.05 hours, 0.5 hours, and 1.0 hours. A) 0.01h, with a mean latitudinal moisture flow of  $1.4^\circ$  in northerly direction and mean longitudinal flow of  $14.3^\circ$  in westerly direction; B) 0.05h, with a mean latitudinal moisture flow of  $1.3^\circ$  in northerly direction and mean longitudinal flow of  $14.2^\circ$  in westerly direction; C) 0.5h, with a mean latitudinal moisture flow of  $1.5^\circ$  in northerly direction and mean longitudinal flow of  $14.4^\circ$  in westerly direction; D) 1.0h, with a mean latitudinal moisture flow of  $1.5^\circ$  in northerly direction and mean longitudinal flow of  $14.5^\circ$  in westerly direction.**



630

635

640

645

**Figure 9: Different footprints of moisture releases from Manaus in July 2012 in a three-dimensional Lagrangian model with different mixing assumptions: without and with accounting for the three-dimensional moisture flows in the ERA5 data (termed omega), and with different assumptions of additional vertical mixing speed (full mixing every 1h, every 6h, every 24, and every 120h). A) Without omega, every 1h mixing, with a mean latitudinal moisture flow of  $2.4^\circ$  in northerly direction and mean longitudinal flow of  $16.4^\circ$  in westerly direction; B) Without omega, every 6h mixing, with a mean latitudinal moisture flow of  $1.4^\circ$  in northerly direction and mean longitudinal flow of  $14.3^\circ$  in westerly direction; C) Without omega, every 24h mixing, with a mean latitudinal moisture flow of  $0.1^\circ$  in northerly direction and mean longitudinal flow of  $11.6^\circ$  in westerly direction; D) Without omega, every 120h mixing, with a mean latitudinal moisture flow of  $1.2^\circ$  in northerly direction and mean longitudinal flow of  $9.0^\circ$  in westerly direction; E) With omega, every 1h mixing, with a mean latitudinal moisture flow of  $3.0^\circ$  in northerly direction and mean longitudinal flow of  $16.7^\circ$  in westerly direction; F) With omega, every 6h mixing, with a mean latitudinal moisture flow of  $0.3^\circ$  in northerly direction and mean longitudinal flow of  $14.5^\circ$  in westerly direction; G) With omega, every 24h mixing, with a mean latitudinal moisture flow of  $5.0^\circ$  in northerly direction and mean longitudinal flow of  $12.3^\circ$  in westerly direction; H) With omega, every 120h mixing, with a mean latitudinal moisture flow of  $6.9^\circ$  in northerly direction and mean longitudinal flow of  $11.5^\circ$  in westerly direction.**